Research Article

Selected Paper from the 6th International Thai Institute of Chemical Engineering and Applied Science Conference (ITIChE2016)

Preparation and Properties of Electrospun Fibers of Titanium Dioxide-loaded Polylactide/Polyvinylpyrrolidone Blends

Bunthoeun Nim, Paiboon Sreearunothai and Pakorn Opaprakasit*
School of Bio-Chemical Engineering and Technology, Sirindhorn International Institute of Technology (SIIT), Thammasat University, Pathum Thani, Thailand

Atitsa Petchsuk
National Metal and Materials Technology Center, Thailand Science Park, Pathum Thani, Thailand

* Corresponding author. E-mail: pakorn@siit.tu.ac.th

DOI: 10.14416/j.ijast.2018.10.003
Received: 18 July 2017; Revised: 20 August 2017; Accepted: 21 August 2017; Published online: 4 October 2018

Abstract

Nanofibers of polylactide (PLA)/polyvinylpyrrolidone (PVP) blends loaded with titanium dioxide (TiO_2) particles have been prepared by an electrospinning technique. TiO_2 particles are formed by sol-gel mechanisms from titanium (IV) iso-propoxide (TTIP) precursor. Effect of TiO_2 formation rate on properties of the fibers are examined by adding iso-propyl alcohol (iPOH) to slow down the TiO_2 precipitation process. The use of iPOH produces fiber mats consisting of slightly bigger and smoother filaments, but smaller-sized embedded TiO_2 particles. Both materials show a distinct UV absorption characteristic of TiO_2 at λ_{max} 300 nm, which can be applied in catalytic applications. Degradation behaviors of the materials in phosphate buffer solutions have also been investigated. The materials have high potential for use as epoxidation catalysts for conversion of vegetable oils to polymeric building blocks and plasticizers.

Keywords: Polylactide, Polyvinylpyrrolidone, Titanium dioxide, Electrospinning, Degradation

1 Introduction

Polylactide (PLA) is one of widely used biodegradable polymers, which can be synthesized from renewable resources. This polymer is derived from lactic acid monomers, commonly obtained from fermentation of agricultural products, such as corn, rice, wheat, and cassava starch [1]. PLA is recently applied in a wide range of applications, including packaging [2], [3], tissue engineering [4], scaffold engineering [5], wound dressing, drug delivery, and anti-microbial materials [6], due to its good mechanical properties, ease of processibility, biodegradability [7], [8], biocompatibility [9], and high transparency [10]. Therefore, the materials is a promising alternate to non-degradable petroleum-based plastics to solve serious plastic waste problems.

Polymer blends and composites have attracted vast attention from the research community and industrial sector to further improve properties of the materials and expand their applications [11], [12]. Various blends and composites of PLA have been developed and used for many specific applications. Recently, composites of PLA with titanium dioxide (TiO_2) particles were prepared and their properties and potentials were examined. TiO_2 nanoparticles possess a unique photocatalytic activity that can be applied in environmental remediation, especially degradation of organic pollutants and bacteria with high efficiency [13]–[15].

Major advantages of using TiO_2 particles include inexpensive cost, non-toxicity, high chemical stability,

Please cite this article as: B. Nim, P. Sreearunothai, P. Opaprakasit, and A. Petchsuk, "Preparation and properties of electrospun fibers of titanium dioxide-loaded polylactide/polyvinylpyrrolidone blends," *Applied Science and Engineering Progress*, vol. 12, no. 1, pp. 52–58, Jan.–Mar. 2019.

and high resistant to solvents. Various preparation methods of TiO_2 and PLA/TiO_2 composites were reported, such as in situ polymerization[16], electrospinning [6], [17], [18], spin coating [19], [20], solution casting [9], and a surface modified method [10]. In addition, several PLA-based blends were used to prepare various composites, including polyvinylpyrrolidone (PVP) [21], polyethylene (PE) [22], polystyrene (PS) [23], and poly(butylene succinate) (PBS) [24]. Among these, PVP shows interesting properties, as it is water soluble, with low toxicity and high physiological compatibility [25]. This polymer is also considered as a conventional polymer for safe use in pharmaceutical, cosmetic, and food industries [26].

There are several reports of PVP carrier in an electrospinning technique. The particles are embedded to the polymer for various applications such as dye degradation [15], [17], sensor [18], and bio-sensing [12].

Blends of PLA and PVP loaded with TiO_2 nanoparticles (PLA/PVP/TiO_2) are a promising nanocomposite for use in improving PLA's properties and introducing specific catalytic activities. These composites exhibited superior properties, compared to their neat material counterparts, such as higher Young's modulus, improved thermal stability, higher photo-degradability and biodegradability, and higher gas barrier properties [27], [28]. Nanocomposite fibers of PLA/TiO_2/PVP/$ZnCl_2$ were fabricated by an electrospinning technique and used in wound dressing applications [21].

In this work, TiO_2-loaded PLA/PVP nanofibers are fabricated by an electrospinning method. The loaded TiO_2 particles are formed by sol-gel mechanisms by employing their precursor solution mixed with the solutions of the polymer matrix during the electrospinning process. Effects of TiO_2 particles formation rate on properties of the fibers are examined by adding isopropyl alcohol. Morphology and properties of the resulting fiber mats are investigated. The materials have high potential for use as catalytic system. Their stability and degradability are then examined in Phosphate Buffer Solutions (PBS), under UVA light activator [29].

2 Methodology

2.1 *Materials*

Polylactide 4043D (PLA) was supplied by NatureWork®. Polyvinylpyrrolidone (PVP) K29-32 (Mw=58,000 g/mol) and Titanium (IV) Iso-propoxide, $Ti(OiPr)_4$ (TTIP), precursor (98+ %) were purchased from Acros. Chloroform RPE (>99%), N,N-dimethyl formamide (DMF) (99.8%), and isopropyl alcohol (99.7%) (iPOH) solvents were purchased from Carlo Erba. Sodium dihydrogen phosphate monohydrate (NaH_2PO_4;H_2O) and disodium hydrogen phosphate heptahydrate (Na_2HPO_4;$7H_2O$) were supplied by Carlo Erba and PANREAC, respectively.

2.2 *Preparation of PLA/PVP blends and TiO_2-loaded composites*

PLA/PVP blends were prepared by mixing PLA (0.84 g) with PVP at a ratio of 5:1 wt/wt, in chloroform (9 g), and stirring until completely dissolved. The TiO_2 precursor mixture was prepared from TTIP (200 µL), mixed with DMF (3 g) and iPOH (1.5 g), followed by adding of DI water (100 µL) drop wise. The mixture was stirred at room temperature for 1 h. iPOH was used to slow down the precipitation rate of TiO_2 particles. The polymer mixture was then mixed with the precursor mixture and stirred at room temperature for 1 h to generate suitable solutions for electrospinning. A summary of the samples compositions and sample names is listed in Table 1.

Table 1: Summary of sample compositions and sample names

Samples	PLA (g)	PVP (g)	TTIP (µL)	iPOH (g)
P-P-T	0.84	0.168	200	0
P-P-I-T	0.84	0.168	200	1.5

2.3 *Electrospinning*

Fiber mats were fabricated by an electrospinning technique. The composited mixture was placed in a syringe (capacity of 3 mL) connected to a syringe-stainless needle. The syringe was placed on a flow controller (KD Scientific KD 100 Syringe Pump), with a flow rate of 1 mL/h. The distance between the collector and the needle tip was 15 cm. A voltage of 10 kV was applied by using a Gamma high voltage (0–40 kV) power supply. The electrospun fibers were gathered on an aluminum foil collector.

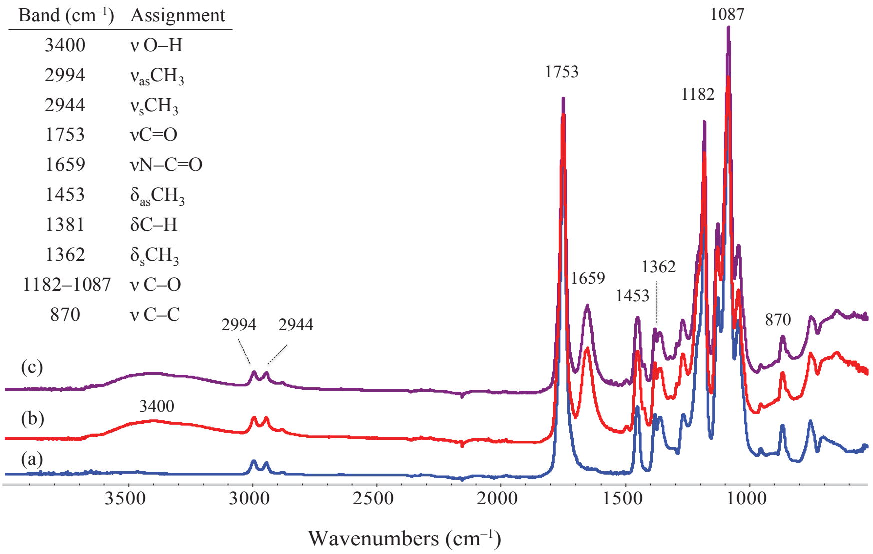

Band (cm^{-1})	Assignment
3400	ν O–H
2994	$\nu_{as}CH_3$
2944	$\nu_{s}CH_3$
1753	νC=O
1659	νN–C=O
1453	$\delta_{as}CH_3$
1381	δC–H
1362	$\delta_{s}CH_3$
1182–1087	ν C–O
870	ν C–C

Figure 1: ATR-FTIR spectra of fiber mats: (a) Neat PLA, (b) P-P-T, and (c) P-P-I-T.

2.4 *Characterization*

Fourier Transform Infrared (FTIR) spectroscopy, equipped with an Attenuated Total Reflectance (ATR) accessory (Nicolet iS5 Spectrometer), was employed to determine functional groups and interactions of the electrospun fiber mats. Scanning electron microscopy (SEM-SU8030) was used to investigate size and surface morphology of the samples. Energy-dispersive X-ray (EDX-SU8030) was employed to observe surface compositions of each component. A UV-Vis spectrophotometer (Genesys 10S) was used to examine the absorption behaviors of the fiber mats.

2.5 *Degradation experiments*

Degradation behaviors of the fiber mats were examined in phosphate buffer solutions (PBS at pH 7.4) at ambient temperature. Neat PLA, P-P-T, and P-P-I-T fiber mats were cut into 2×2 cm^2. Each specimen was immersed into 50 mL PBS and placed at a 22 cm distance under UVA light (UVA 15WT8 lamp). The experiments were conducted for 6 days, in which the specimens were removed from the solution and washed with DI water and dried at 40°C in a vacuum oven for overnight. FTIR and UV-Vis spectroscopy were used to examine the chemical structures of the samples as a function of degradation time.

3 Results and Discussion

3.1 *ATR-FTIR spectroscopy*

ATR-FTIR spectra of spun fiber samples of neat PLA, P-P-T, and P-P-I-T are shown in Figure 1. Band characteristics of PLA and PVP are observed, indicating the presence of the 2 components on a filament's surface. A strong band at 1,753 cm^{-1} is assigned to the vibration of C=O of PLA chains, whereas that at 1,659 cm^{-1} corresponds to the amide (N-C=O) vibrational mode. Both P-P-T and P-P-I-T show similar FTIR spectra pattern. This reflects that the technique may not be able to differentiate the nature of the two samples. Nonetheless, a broad band centered at 3,400 cm^{-1} (O-H stretching), observed in these 2 samples but not in neat PLA, indicates the presence of remaining iPOH after the TiO_2 particle formation, and also bound water molecules due to the hygroscopic nature of PVP.

3.2 *Scanning electron microscopy*

Figure 2 shows surface morphology of P-P-T and P-P-I-T mats examined by SEM. Significant differences between the 2 samples are observed. Both sample mats show rough and irregular surface morphology, which is different from that of neat PLA, as reported earlier [30]. This is likely due to the interplay between

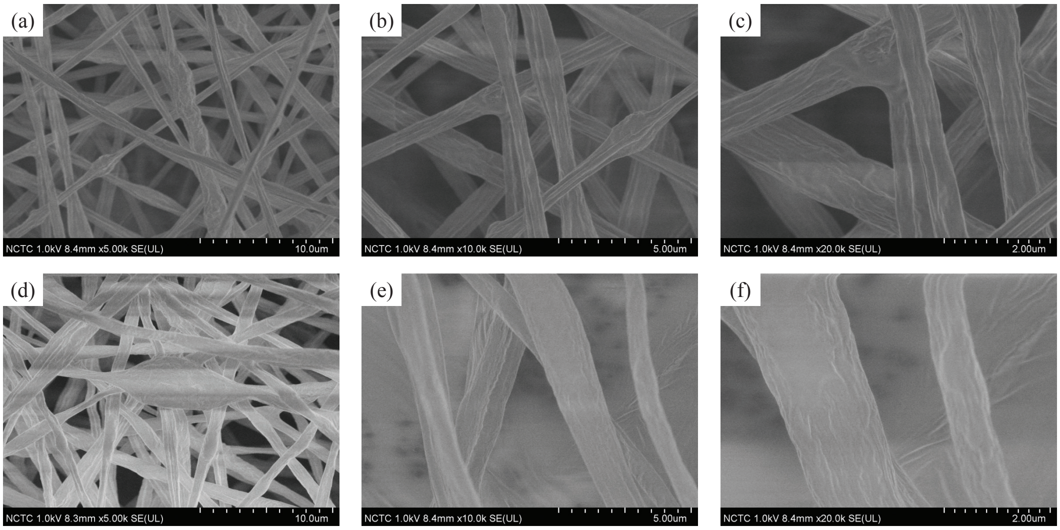

Figure 2: SEM images of electrospun fibers (a)–(c) P-P-T and (d)–(f) P-P-I-T at 5,000×, 10,000×, and 20,000× magnifications.

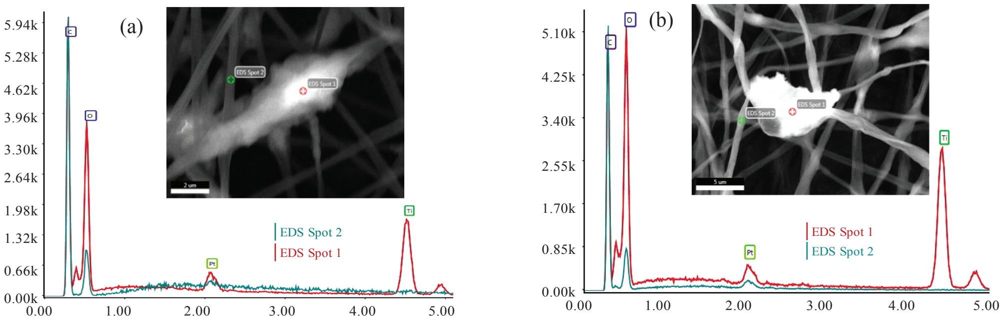

Figure 3: EDX spectra illustrating atomic compositions of bead defects with different sizes present in (a) P-P-T and (b) P-P-I-T fibers.

the 2 polymeric components during electrospinning. Nonetheless, it is clearly observed that the surface of P-P-I-T fibers is smoother than that of P-P-T. The fiber mats of P-P-I-T contains TiO_2 beads with higher uniformity than those of P-P-T, as the addition of iPOH slows down the TiO_2 precipitation rate. The regions of irregular fiber (beads) shape are caused by agglomeration of TiO_2 particles present as beads embedded in the filaments. This is confirmed by EDX results, as illustrated in Figure 3. The Ti content in the beads is much higher, compared to that in the regular fiber region. The size distribution of the filaments is compared in Figure 4. The P-P-T fibers have an average diameter of 800 nm, slightly smaller than that of P-P-I-T (827 nm).

3.3 *UV-Vis spectroscopy*

UV-Vis spectroscopy is employed to examine absorption behaviors of the materials, as shown in Figure 5. P-P-T and P-P-I-T fibers show a major absorption band at λ_{max} 214 nm. This is due to the $n \rightarrow \pi^*$ transition of the carbonyl groups in PLA, which is similar to that observed in spun fibers of neat PLA. All samples also show a broad absorption covering the full visible region, likely due to the translucent nature of the fiber mats. A distinct absorption band is observed at 300 nm for P-P-T and P-P-I-T fiber mats, indicating the presence of TiO_2 particles. This enables the materials to possess photo-catalytic activity for use in many applications, such as epoxidation of unsaturated oils or degradation

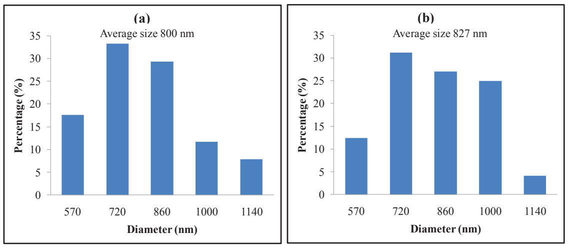

Figure 4: Size distribution of (a) P-P-T and (b) P-P-I-T fiber mats.

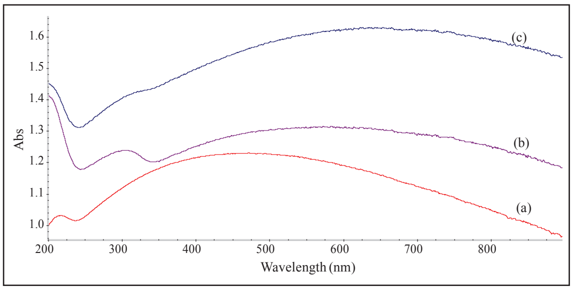

Figure 5: UV-Vis spectra of fibers mats of: (a) neat PLA, (b) P-P-T, and (c) P-P-I-T.

of contaminated water. Due to space limitations, this will be addressed in details in a separate work.

3.4 *Degradation mechanisms*

Degradation behaviors of the spun fiber mats are examined in PBS solutions by activation with UVA light. The fiber samples were soaked in PBS at 1, 4, and 6 days, and their FTIR and UV-Vis spectra were recorded, as shown in Figure 6. The ATR-FTIR and UV-Vis results show evidences of PLA degradation as a function of time, similar to those reported in our previous work [31]. Both P-P-T and P-P-I-T mats show similar FTIR changes, and the latter is chosen to show the changes. A decrease in intensity of the 1659 cm^{-1} band of the amide group of PVP reflects that during the degradation, PVP present on the surface of the filaments is released and dissolves in PBS solutions. In addition, a weak band in the same region is observed at 1,650 cm^{-1}, associated with carboxylate of degraded PLA.

Results from UV-Vis spectra of PBS solutions after P-P-I-T fiber mats are soaked for 1, 4, and 6 days, as shown in Figure 7, illustrates an absorption band of lactate oligomers, products from the degradation of PLA, at 202 nm. The intensity of the band increases with the degradation time, indicating that degradation of the PLA component takes place very early. This is likely because of the presence of TiO$_2$ catalytic particles and the dissolubility of PVP from the filaments, which in turn, exposes the PLA component to a higher degree of hydrolysis.

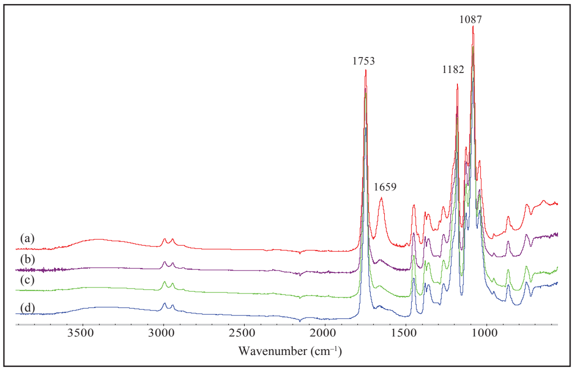

Figure 6: ATR-FTIR spectra of electrospun P-P-I-T (10 kV) fiber soaked in PBS solution at: (a) 0, (b) 1, (c) 4, and (d) 6 days.

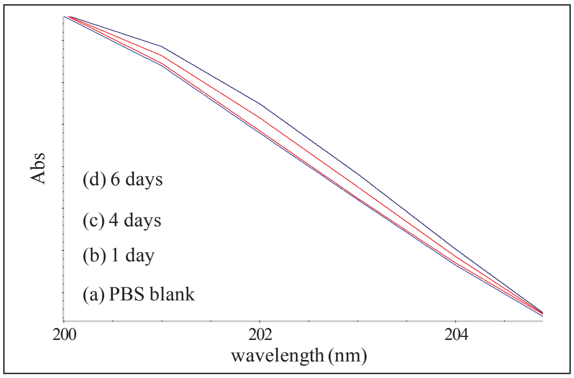

Figure 7: UV-Vis spectra of P-P-I-T fiber mats as a function of degradation time: 1, 4, and 6 days.

4 Conclusions

Fiber mats of PLA/PVP blends loaded with TiO$_2$ particles, i.e., P-P-T, and P-P-I-T, are successfully fabricated by an electrospinning method. The fiber mats absorb UV light in a region of 300 nm, which enables their photo-catalytic activity. Preliminary results from degradability experiments show that degradation of the PLA component takes place very early, due to the presence of TiO_2 catalytic particles and the dissolubility of PVP from the filaments.

Acknowledgements

The authors acknowledge financial supports from the Thammasat University Research Fund (Theme research) and the Center of Excellence in Materials and Plasma Technology (M@P Tech), Thammasat University. B.N. thanks the support from the Excellence Foreign Scholarship (EFS) program provided by SIIT. The authors would like to convey special appreciation to the academic committee of The 6th International Thai Institute of Chemical Engineering and Applied Science Conference (ITIChE2016) for providing the opportunity for this work to be published in this journal.

References

[1] T. Mekonnena, P. Mussonea, H. Khalilb, and D. Bressler, “Progress in bio-based plastics and plasticizing modifications,” *Journal of Materials Chemistry A*, vol. 1, pp. 13379–13398, 2013.

[2] F. Carosio, S. Colonna, A. Fina, G. Rydzek, J. Hemmerlé, L. Jierry, P. Schaaf, and F. Boulmedais, “Efficient gas and water vapor barrier properties of thin poly(lactic acid) packaging films: Functionalization with moisture resistant nafion and clay multilayers,” *Chemistry of Materials*, vol. 26, no. 19, pp. 5459–5466, 2014.

[3] G. Colomines, V. Ducruet, C. Courgneau, A. Guinault, and S. Domenek, “Barrier properties of poly(lactic acid) and its morphological changes induced by aroma compound sorption,” *Polymer International*, vol. 59, no. 6, pp. 818–826, 2010.

[4] F. G. Torres, S. N. Nazhat, S. H. Sheikh Md Fadzullah, V. Maquetd, and A. R. Boccaccini, “Mechanical properties and bioactivity of porous PLGA/TiO_2 nanoparticle-filled composites for tissue engineering scaffolds,” *Composites Science and Technology*, vol. 67, no. 6, pp. 1139–1147, 2007.

[5] A. Buzarovska, C. Gualandi, A. Parrilli, and M. Scandola, “Effect of TiO_2 nanoparticle loading on poly(l-lactic acid) porous scaffolds fabricated by TIPS,” *Composites Part B: Engineering*, vol. 81, pp. 189–195, 2015.

[6] K. K. Gupta, P. K. Mishra, P. Srivastava, M. Gangwar, G. Nath, and P. Maiti, “Hydrothermal in situ preparation of TiO_2 particles onto poly(lactic acid) electrospun nanofibres,” *Applied Surface Science*, vol. 264, pp. 375–382, 2013.

[7] G. Kale, R. Auras, S. P. Singh, and R. Narayan, “Biodegradability of polylactide bottles in real and simulated composting conditions,” *Polymer Testing*, vol. 26, no. 8, pp. 1049–1061, 2007.

[8] K. Fukushima, C. Abbate, D. Tabuani, M. Gennari, and G. Camino, “Biodegradation of poly(lactic acid) and its nanocomposites,” *Polymer Degradation and Stability*, vol. 94, no. 10, pp. 1646–1655, 2009.

[9] A. Buzarovska and A. Grozdanov, “Biodegradable poly(L-lactic acid)/TiO_2 nanocomposites: Thermal properties and degradation,” *Journal of Applied Polymer Science*, vol. 123, no. 4, pp. 2187–2193, 2012.

[10] N. Nakayama and T. Hayashi, “Preparation and characterization of poly(l-lactic acid)/TiO_2 nanoparticle nanocomposite films with high transparency and efficient photodegradability,” *Polymer Degradation and Stability*, vol. 92, no. 7, pp. 1255–1264, 2007.

[11] P. Singh, K. Mondal, and A. Sharma, “Reusable electrospun mesoporous ZnO nanofiber mats for photocatalytic degradation of polycyclic aromatic hydrocarbon dyes in wastewater,” *Journal of Colloid and Interface Science*, vol. 394, pp. 208–215, 2013.

[12] K. Mondal, M. A. Ali, V. V. Agrawal, B. D. Malhotra, and A. Sharma, “Highly sensitive biofunctionalized mesoporous electrospun TiO_2 nanofiber based interface for biosensing,” *ACS Applied Materials & Interfaces*, vol. 6, no. 4, pp. 2516–2527, 2014.

[13] W.-C. Lin, W.-D. Yang, and S.-Y. Jheng, “Photocatalytic degradation of dyes in water using porous nanocrystalline titanium dioxide,” *Journal of the Taiwan Institute of Chemical Engineers*, vol. 43, pp. 269–274, 2012.

[14] C. Chawengkijwanich and Y. Hayata, “Development of TiO_2 powder-coated food packaging film and its ability to inactivate *Escherichia coli* in vitro and in actual tests,” *International Journal of Food Microbiology*, vol. 123, pp. 288–292, 2008.

[15] N. Singh, K. Mondal, M. Misra, A. Sharmaab, and R. K. Gupta, “Quantum dot sensitized electrospun mesoporous titanium dioxide hollow nanofibers for photocatalytic applications,” *RSC Advances*, vol. 6, no. 53, pp. 48109–48119, 2016.

[16] M. A. Ali, K. Mondal, Y. Wang, H. Jiang, N. K. Mahal, M. J. Castellano, A. Sharma, and L. Dong, “*In situ* integration of graphene foam-titanium nitride based bio-scaffolds and microfluidic structures for soil nutrient sensors,” *Lab on a Chip*, vol. 17, no. 2, pp. 274–285, 2017.

[17] K. Mondal, S. Bhattacharyya, and A. Sharma, “Photocatalytic degradation of naphthalene by electrospun mesoporous carbon-doped anatase TiO_2 nanofiber mats,” *Industrial & Engineering Chemistry Research*, vol. 53, no. 49, pp. 18900–18909, 2014.

[18] Md. A. Ali, K. Mondal, Y. Jiao, S. Oren, Z. Xu, A. Sharma, and L. Dong, “Microfluidic immuno-biochip for detection of breast cancer biomarkers using hierarchical composite of porous graphene and titanium dioxide nanofibers,” *ACS Applied Materials & Interfaces*, vol. 8, no. 32, pp. 20570–20582, 2016.

[19] C. Man, C. Zhang, Y. Liu, W. Wang, W. Ren, L. Jiang, F. Reisdorffer, T. P. Nguyen, and Y. Dan, “Poly (lactic acid)/titanium dioxide composites: Preparation and performance under ultraviolet irradiation,” *Polymer Degradation and Stability*, vol. 97, no. 6, pp. 856–862, 2012.

[20] K. Mondal, J. Kumar, and A. Sharma, “TiO_2-nanoparticles-impregnated photocatalytic macroporous carbon films by spin coating,” *Nanomaterials and Energy*, vol. 2, no. 3, pp. 121–133, 2013.

[21] Y. Hong, Y. Li, X. Zhuang, X. Chen, and X. Jing, “Electrospinning of multicomponent ultrathin fibrous nonwovens for semi-occlusive wound dressings,” *Journal of Biomedical Materials Research Part A*, vol. 89, no. 2, pp. 345–354, 2009.

[22] K. I. M. da Silva, J. A. Fernandes, E. C. Kohlrausch, J. Dupont, M. J. L. Santos, and M. P. Gil, “Structural stability of photodegradable poly(l-lactic acid)/PE/TiO_2 nanocomposites through TiO_2 nanospheres and TiO_2 nanotubes incorporation,” *Polymer Bulletin*, vol. 71, no. 5, pp. 1205–1217, 2014.

[23] N. G. Shimpi, M. Borane, and S. Mishra, “TiO_2/polystyrene core–shell nanoparticles as fillers for LLDPE/PLA blend: Development, and morphological, thermal and mechanical properties,” *Polymer Bulletin*, vol.73, no. 11, Nov. 2016.

[24] A. Buasri, G. Buranasing, R. Piemjaiswang, S. Yousatit, and V. Loryuenyong, “Effect of titanium dioxide nanoparticles on mechanical and thermal properties of poly(lactic acid) and poly(butylene succinate) blends,” *Advances in Science and Technology*, vol. 96, pp. 33–38, 2014.

[25] C. N. Hsiao and K. S. Huang, “Synthesis, characterization, and applications of polyvinylpyrrolidone/SiO_2 hybrid materials,” *Journal of Applied Polymer Science*, vol. 96, no. 5, pp. 1936–1942, 2005.

[26] F. Haaf, A. Sanner, and F. Straub, “Polymers of N-Vinylpyrrolidone: Synthesis, characterization and uses,” *Polymer Journal*, vol. 17, no. 1, pp. 143–152, 1985.

[27] W. Zhuang, J. Liu, J. H. Zhang, B. X. Hu, and J. Shen, “Preparation, characterization, and properties of TiO_2/PLA nanocomposites by in situ polymerization,” *Polymer Composites*, vol. 30, no. 8, pp. 1074–1080, 2009.

[28] N. A. Ali and F. T. M. Noori, “Gas barrier properties of biodegradable polymer nanocomposites films,” *Chemistry and Materials Research*, vol. 6, no. 1, pp. 44–51, 2014.

[29] Y.-B. Luo, X.-L. Wang, and Y.-Z. Wang, “Effect of TiO_2 nanoparticles on the long-term hydrolytic degradation behavior of PLA,” *Polymer Degradation and Stability*, vol. 97, no. 5, pp. 721–728, 2012.

[30] C. Thammawong, S. Buchatip, A. Petchsuk, P. Tangboriboonrat, N. Chanunpanich, M. Opaprakasit, P. Sreearunothai, and P. Opaprakasit, “Electrospinning of poly(l-lactide-co-dl-lactide) copolymers: Effect of chemical structures and spinning conditions,” *Polymer Engineering and Science*, vol. 54, no. 2, pp. 472–480, 2014.

[31] P. Sriromreun, A. Petchsuk, M. Opaprakasit, and P. Opaprakasit, “Standard methods for characterizations of structure and hydrolytic degradation of aliphatic/aromatic copolyesters,” *Polymer Degradation and Stability*, vol. 98, no. 1, pp. 169–176, 2013.